

Coating of Glass and Polycarbonate with Aqueous Two-Component Polyurethane Resin

Massimiliano Barletta,¹ Silvia Pezzola,¹ Vincenzo Tagliaferri,¹ Federica Trovalusci²

¹Dipartimento di Ingegneria dell'Impresa, Università degli Studi di Roma Tor Vergata, Via del Politecnico 1, 00133 Roma, Italy

²Università degli Studi Niccolò Cusano - Telematica Roma, Via Don Carlo Gnocchi 3, 00166 Roma, Italy

Correspondence to: M. Barletta (E-mail: barletta@ing.uniroma2.it)

ABSTRACT: Hard polyurethane coatings combine several features as high flexibility and toughness, good chemical resistance, improved clarity, and spontaneous air-drying. However, the coating design (thicknesses, interface pretreatments, substrate features, etc.) is often troublesome. In this respect, the present investigation deals with the application of high-clarity polyurethane coatings on transparent glass and polycarbonates. In particular, the role of the coating thicknesses and, above all, of the different compliance of the substrates was investigated. Progressive mode scratch and dry sliding linear reciprocating tribological tests were carried out and scanning electron microscopy images were captured to analyze the deformation response of the polyurethane coatings. The experimental findings allow to better interpret the way to ruptures of the investigated coating systems and the mechanisms involved. Accordingly, new strategies to prevent them could be elicited. © 2013 Wiley Periodicals, Inc. *J. Appl. Polym. Sci.* **2014**, *131*, 40021.

KEYWORDS: coatings; friction; wear and lubrication; manufacturing; mechanical properties; surfaces and interfaces

Received 20 August 2013; accepted 30 September 2013

DOI: 10.1002/app.40021

INTRODUCTION

Hard polyurethanes are widely used as surface overlaying coatings on a large variety of substrates for their formidable combination of properties, as high flexibility and toughness, good chemical resistance, improved clarity and spontaneous air-drying. Waterborne two-component polyurethane (2K-PUR) coatings have always been the matter of extensive investigations.^{1,2} In 1997, in a climate of growing concerns due to the increased restriction on volatile organic compounds in coatings, Noble described the advantages of waterborne one-component polyurethanes and reactive two-component systems as environmentally friendly alternative to solventborne resin.¹ In 2000, Melchioris et al. attempted to systematize the potentiality of the polyurethane coatings, with a special focus on the environmental compliant waterborne 2K-PUR coatings. They explained the key to industrial viability of the waterborne polyurethanes relied on the presence in the polyurethane chains of the urethane groups, known to be resistant to aggressive chemicals, and by the high density of hydrogen bridge bonds, known to confer to the resin high stability and outstanding mechanical properties.² The additional route to the industrial viability of the polyurethanes was their intrinsic flexible design.³ Madbouly and Otaigbe³ showed how polyurethanes can be tailored, thus allowing the customization of their chemical formulation by the modulation of the soft (i.e., polyether, polyester or polycarbon-

ate) and hard (i.e., the density of the physical network determined by the hydrogen bridge bonds and other chemical interactions) segments of the polymeric network. Besides, polyurethanes could also be customized according to the final molecular weight of the resin, the degree of branching of the polymeric chains and/or the incorporation in the network of other groups which can modify properties like the hydrophobicity, the ability to cross-link as well as the final aesthetic and functional effects after resin deposition and drying as detailed in Ref. 4.

Experimental efforts spent in the last decades on polyurethanes have pushed their widespread usages as clear topcoat on a wide range of commodities like interior and exterior automotive components, consumer electronics, sporting equipments, safety helmets to name a few.⁵ However, some drawbacks do still limit the market potential of polyurethanes. In particular, intensive stresses on polyurethane coatings can easily provoke significant mar and scratch damage in short order.⁵⁻⁷ In addition, most of the solutions implemented to confer extra resistance to polyurethanes are by introducing in their formulations inorganic fillers or moieties through the design of organic-inorganic hybrid materials via the sol-gel route,⁴ which is often difficult to manage and implement on large-scaled industrial process.^{4,6,7} Moreover, being the inorganic fillers highly refractive, they can often compromise the high clarity of the polyurethane coatings and

reduce the aesthetic appeal of the underlying substrates.⁸ However, the achievement of the proper performance of the polyurethane coating systems is often not related to chemistry and material design. High performance is frequently compromised by the poor knowledge of several practical issues concerning the manufacturing process of the coatings like, for example, the correct thickness to apply, the physical-chemical interaction of the polyurethanes with the underlying materials and, above all, the compliance of the substrates as emphasized in Ref. 9.

In this respect, the present investigation deals with the application of high-clarity polyurethane coatings on transparent glass and polycarbonates. In particular, the role of the coating thicknesses, and, above all, of the different compliance of the substrates was investigated. Progressive mode scratch and dry sliding linear reciprocating tribological tests were carried out and scanning electron microscopy (SEM) images were captured to analyze the deformation response of the polyurethane coatings. The experimental findings allow to better interpret the way to ruptures of the investigated coating systems and the mechanisms involved. Accordingly, new strategies to prevent coating failures and viable solutions to the manufacturing of high-resistant polyurethane coatings could be elicited.

EXPERIMENTAL

Materials

The polyurethane resin is based on a two-component branched hydroxyl-bearing polyester with aliphatic polyisocyanate based on hexamethylene diisocyanate (Bayer-coating; Bayer MaterialScience AG, Brunsbüttel, Germany). The substrates (25 mm × 80 mm) on which the resin was deposited were cut off from commercially available float glass (300 mm × 100 mm, 3 mm in thickness) and polycarbonate sheets (2000 mm × 1000 mm, 3 mm in thickness).

Coating Process

Before the deposition process of the polyurethane resin, the different substrates were submitted to pretreatments aimed at maximizing the adhesion of the overlying coating. The glass substrate was chemically corrugated by a commercially available etching paste (Idea Glass, Maimeri spa, Mediglia, MI, Italy). The etching lasted 30 min and, then, the paste was washed out by rinsing with demineralized water and drying at room temperature. The polycarbonate substrates were only washed with a diluted solution of isopropyl alcohol, rinsed with demineralized water and dried at room temperature.

The coating was formulated by diluting the hydroxyl-bearing polyester resin in 2-butanone in a ratio of 1 : 1 (w/w). The resulting solution was put under magnetic stirring until homogeneity was achieved. Hexamethylene diisocyanate was added dropwise, whilst keeping the mixture under stirring for approximately 15 min. The formulation was, thus, deposited on the substrates by spraying or automatic drawdown applicator (ADA; Automatic Film Applicator L, BYK-Gardner, Germany). Spraying process was carried out by an air-mix gun equipped with a nozzle of 0.8 mm and setting the feeding pressure at ~1.75 bar. ADA was carried out by setting the applicator speed at 0.5 m/

min. After the deposition, the coated substrates were left for 100 h in a climatic chamber (Binder KBF240; Binder GmbH, Tuttlingen, Germany) at $40 \pm 2\%$ relative humidity (RH) and $20 \pm 0.2^\circ\text{C}$ temperature to allow the drying of the resin.

Coating Characterization

The coatings were analyzed by field-emission gun-scanning electron microscope (FEG-SEM Leo Supra 35, Cambridge, UK) using both the secondary electrons and in-lens detectors and by a contact gauge Taylor Hobson Surface Topography System (TalySurf CLI 2000; Taylor Hobson, Leicester, UK), using the intermediate range mode (2.3 mm). The surface roughness was analyzed by recording a number of patterns (10), each 20 mm long, to cover an area 20 mm × 5 mm. 1000 points per mm were stored along the measurement directions. TalyMap software Release 3.1 was used to get the roughness parameters and, in particular, the standard amplitude, spacing and hybrid parameters (Gaussian filter, 0.8 mm). Chemically etched glass showed a R_a of $\sim 1 \mu\text{m}$. As-received polycarbonate was characterized by an average roughness of $\sim 0.25 \mu\text{m}$. The coatings showed lower R_a of ~ 0.35 and $\sim 0.2 \mu\text{m}$ on glass and polycarbonate, respectively.

The thickness of the coatings deposited on the polycarbonate was measured using a magnetic inductive gauge (Mega-Check 5FN-ST; List-Magnetik, Echterdingen, Germany). Instead, the thickness of the coatings deposited on the glass substrates was measured using a digital palmer (Mitutoyo IP65, Kawasaki, Japan). To ensure data reliability, the measurements were performed on five different points equally spaced over the substrate surface. The thicknesses of the coatings were controlled to approach $\sim 75 \pm 15 \mu\text{m}$ after spraying and $\sim 150 \pm 30 \mu\text{m}$ after ADA, respectively.

Coating hardness was measured by pencil test (Scratch Hardness Tester Model 291; Erichsen Testing Equipment, Hemer, Germany). Polyurethane coatings showed a pencil grade of 5–6H, whilst the as-received polycarbonate a mere 2B. As-received glass was not affected by a pencil test performed with a 9H tip.

Micromechanical and Tribological Characterization

Scratch tests on the coatings were performed using a microscale scratch tester (CSM micro-Combi Tester, Peseaux, Switzerland). Scratching was carried out with three variants of Rockwell C-type conical indenter with a rounded tip (100–200 and 800 μm tip radius), operating in progressive mode (pattern 3 mm, scratch speed 1 mm/min, load 30 mN to 30 N) at $\sim 20^\circ\text{C}$ ($\pm 0.2^\circ\text{C}$) and 40% RH along a pattern 3 mm long. The surface imaging tool used to study the shape of residual deformation after scratch tests was the FEG-SEM.

Tribological tests with linear reciprocating dry-sliding motion were performed by a standard tribometer (Tribometer; C.S.M. Instruments, Peseaux, Switzerland) at about 20°C ($\pm 0.2^\circ\text{C}$) and 40% ($\pm 2\%$) RH. The coatings were tested at 5 N load (frequency 3 Hz, sliding distance 10, 25, 50, 100, 200, 500, and 1000 m, and pattern 6 mm long) of the upper Al_2O_3 ball (6 mm diameter). The surface imaging tool used to study the shape of residual wear pattern after the tribological tests was the FEG-SEM. Wear rate of the coatings was assessed by the contact

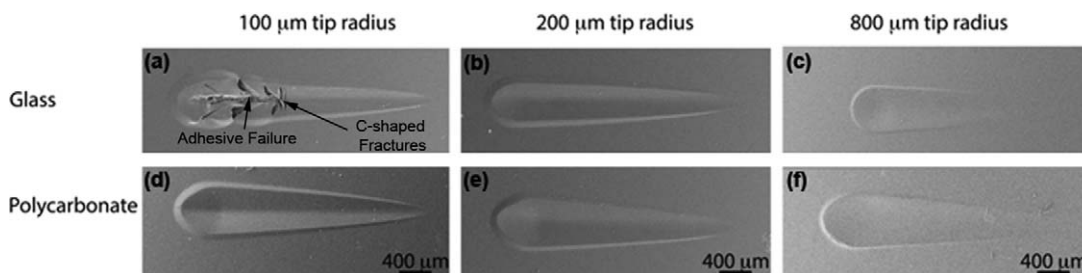


Figure 1. SEM images of the residual scratch patterns after progressive mode scratch tests on the thinner $\sim 75 \mu\text{m}$ polyurethane coatings: (a) glass, $100 \mu\text{m}$ tip radius; (b) glass, $200 \mu\text{m}$ tip radius; (c) glass, $800 \mu\text{m}$; (d) polycarbonate, $100 \mu\text{m}$ tip radius; (e) polycarbonate, $200 \mu\text{m}$ tip radius; and (f) polycarbonate, $800 \mu\text{m}$ tip radius.

probe surface profiler (lateral resolution, $5 \mu\text{m}$), measuring the area involved by the action of the counterpart, the wear volume and the minimum and maximum height of the wear pattern as well as the friction coefficient.

RESULTS AND DISCUSSION

Analysis of the Residual Scratch Pattern

Figures 1 and 2 show the SEM images of the residual scratch patterns of the polyurethane coatings deposited on glass and polycarbonate. In Figure 1, the scratch responses of the thinner $\sim 75 \mu\text{m}$ coatings are reported. The coatings deform permanently under the action of the scratching indenter, whatever indenter tip radii (i.e., 100 , 200 , and $800 \mu\text{m}$) are involved. The permanent deformation is characterized by a growing ditch, whose shape follows the incremental load imposed during the progressive mode scratch tests, surrounded by an accumulation of coating material plastically displaced sideways and in the front of the last contact position between the indenter and the coating itself (i.e., side and front pileup). Increasing the contact pressure during the scratch test, that means, reducing the radius of the indenter tip leads to bigger residual scratch patterns on the coatings deposited on both glass and polycarbonate. However, coating failure only takes place on the polyurethane coating deposited on the glass substrate, when indented with the sharpest $100 \mu\text{m}$ tip radius indenter [Figure 1(a)]. The onset of coating fracture occurs after $\sim 1.8 \text{ mm}$ sliding distance, that is, at $\sim 18 \text{ N}$ normal load. Leftwards C-shaped fractures arise and they are distributed along the scratch pattern for sliding distance over $\sim 1.8 \text{ mm}$. The size of the C-shaped fractures increases at any time the applied normal load grows up during

the progressive mode scratch test. C-shaped fractures on a large variety of coatings are described in the literature¹⁰ and they are the result of the tensile cracking mechanism. Indeed, when the indenter tip slides over the coating surface during a progressive mode scratch test, it imposes an incremental load. The coating material ahead the indenter tip would thus be submitted to a compressive stress field, whereas a tensile stress would act at the back of their actual contact.¹¹ When the tensile stress is over the ultimate tensile strength of the coating material or, alternative, when the tensile stress field extends over the whole thickness, approaching the interface with the underlying substrate and overcoming adhesive toughness, the coating can exhibit brittle failure events. C-shaped fractures depart at the back of the true contact between indenter and coating surface, initiate in the middle of the scratch pattern where the applied load is maximum and propagate sideways. In Figure 1(a), the observed C-shaped fractures remain, however, confined inside the residual scratch pattern. No brittle spallation or buckling¹⁰ are thus characterizing the polyurethane coatings investigated. Nevertheless, Figure 1(a) shows an additional failure mechanism. It initiates at a higher sliding distance (i.e., at higher load) of $\sim 2.25 \text{ mm}$ and it is a sort of isolated linear furrow at the very middle of the scratch pattern. The linear furrow develops in the same direction of the advancing indenter and stops in the last contact position between the indenter tip and the coating surface. It is surrounded by very small side ridges of plastically deformed coating material. The onset of the linear furrow can be interpreted as the result of the indenter tip which, at high load, penetrates the softer coating material, approaching the interface with the underlying harder and stiffer substrate. In

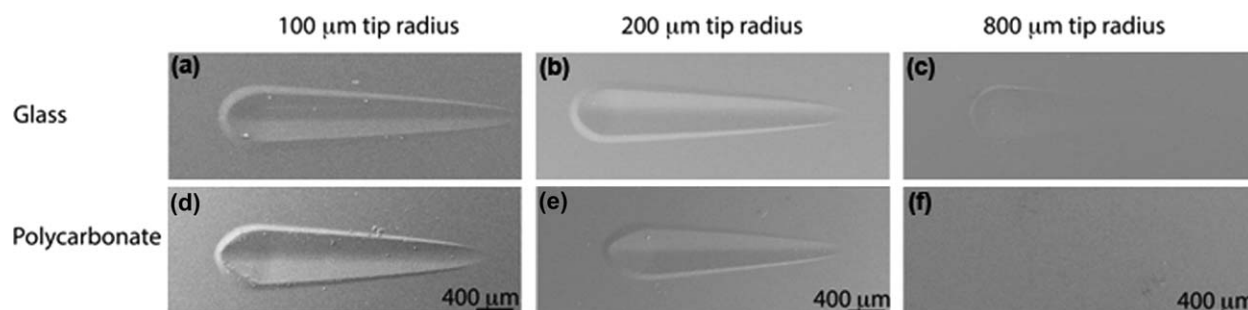


Figure 2. SEM images of the residual scratch patterns after progressive mode scratch tests on the thicker $\sim 150 \mu\text{m}$ polyurethane coatings: (a) glass, $100 \mu\text{m}$ tip radius; (b) glass, $200 \mu\text{m}$ tip radius; (c) glass, $800 \mu\text{m}$; (d) polycarbonate, $100 \mu\text{m}$ tip radius; (e) polycarbonate, $200 \mu\text{m}$ tip radius; and (f) polycarbonate, $800 \mu\text{m}$ tip radius.

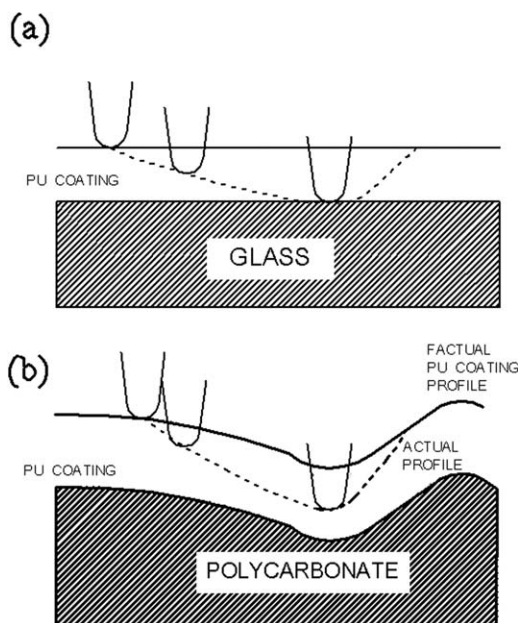


Figure 3. Interaction between the 100 μm indenter and the thinner ~ 75 μm polyurethane coatings during progressive mode scratch test: (a) failure mechanism on glass and (b) mere plastic deformation on polycarbonate.

Figure 1(a), the indenter tip penetrates across the whole coating thickness, approaching the underlying rigid and nearly not deformable glass [Figure 3(a)]. Accordingly, the indenter acts like a cutting tool which causes the coating breakage and the concurrent adhesive failure at the interface with the nearly unaffected underlying glass substrate. This mechanism is partially described by Bautista et al.,¹² which, in their investigation, showed the failure events at lower loads of pretty thinner organic–inorganic hybrid coatings deposited on float glasses. Needless to say that the aforementioned mechanism requires many concurrent events to trigger: (i) penetration depth comparable with the coating thickness; (ii) sharp enough indenter tip and elevated contact pressure; and (iii) coating softer than the stiffer and not compliant at all underlying substrate. These conditions are simultaneously

verified during the progressive mode scratch test of the polyurethane coating on the glass substrate, when it is performed with the indenter tip of 100 μm . Therefore, the indenter generates the breakage of the outermost layer of the coating material at high load and, penetrating it through the entire coating thickness, causes the rupture of the adhesive bonds at the interface between coating and substrate as the imposed cutting force overcomes the interfacial adhesive strength. These events are not simultaneously verified when the polyurethane coatings are deposited on the polycarbonate, as better depicted in Figure 3(b). In Figure 2, the scratch responses of the thicker ~ 150 μm coatings are reported. The influence of the coating thickness is remarkable. The thicker coatings are found to withstand better the action of the sliding indenter during the progressive mode scratch tests. In particular, the polyurethane coatings deposited on polycarbonate do not show any residual scratch pattern when the blunter 800 μm tip radius indenter is used. When the coating is deposited on glass, the onset of scratch visibility (that is, the onset of a permanent deformation on the scratched surface¹³) after progressive mode scratch tests with the blunter 800 μm tip radius indenter is detected at pretty high sliding distance (i.e., applied load) of ~ 2.25 mm. When the sharper (100 and 200 μm radii) indenter tips are used, the onset of scratch visibility is at very low load. However, no fracture events can be detected, neither on glass substrates and for the highest contact pressure.

Analysis of the Scratch Deformation Response

Figures 4 and 5 report the trends of penetration and residual depths of the polyurethane coatings deposited on glass and polycarbonate. In Figure 4, the deformation responses of the thinner ~ 75 μm coatings are reported. The trends of the penetration depth are increasing and follow approximately a power law. The penetration depth depends on the intrinsic properties of the coating and substrate material. Polyurethane coatings deposited on polycarbonates deform more during the application of the scratch load. The maximum penetration depth depends on the tip radius of the indenter. When the sharpest 100 μm tip radius indenter is used, maximum depth of penetration averages ~ 140 μm . The maximum depth of penetration in case of the blunt contact condition with the 800 μm

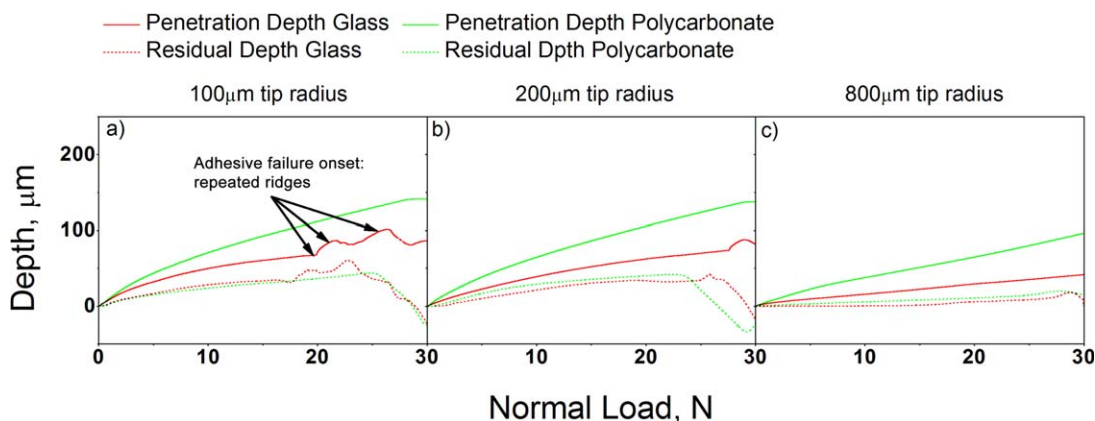


Figure 4. Trend of the penetration and residual depths after progressive mode scratch tests on the thinner ~ 75 μm polyurethane coatings: (a) 100 μm tip radius; (b) 200 μm tip radius; and (c) 800 μm tip radius. [Color figure can be viewed in the online issue, which is available at wileyonlinelibrary.com.]

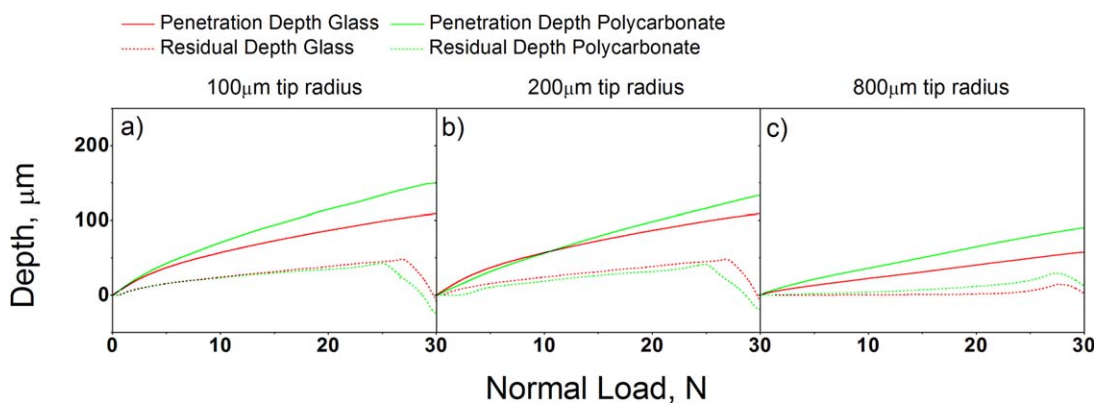


Figure 5. Trend of the penetration and residual depths after progressive mode scratch tests on the thicker $\sim 150 \mu\text{m}$ polyurethane coatings: (a) $100 \mu\text{m}$ tip radius; (b) $200 \mu\text{m}$ tip radius; and (c) $800 \mu\text{m}$ tip radius. [Color figure can be viewed in the online issue, which is available at wileyonlinelibrary.com.]

tip radius indenter averages $\sim 80\text{--}85 \mu\text{m}$. In the former case, the penetration depth is well over the coating thickness. This does not mean that the indenter penetrates the coating material all the way down until the underlying substrate is approached. To the contrary, this is an estimate of the deformation extent of the underlying polycarbonate. Polycarbonate is a ductile and high-flexible plastic, with a moderate stiffness. It is thus extremely compliant when submitted to the action of a scratching indenter and the corresponding localized load. This means the deformation imposed by the indenter on the coating material is partially transferred to the underlying substrate, which, being extremely compliant, tends to deform a lot, complying with the action of the penetrating indenter. Glass substrates behave differently. They are stiffer and nearly not compliant at all. When indented with the sharpest tip, the polyurethane coatings on glass are characterized by a lower maximum penetration depth of approximately $80\text{--}85 \mu\text{m}$. The maximum penetration depth in case of the blunt contact condition with the $800 \mu\text{m}$ indenter is, indeed, a mere $\sim 35\text{--}40 \mu\text{m}$. In the former case, the penetration depth is next to the coating thickness. Indeed, penetration depths comparable with the coating thickness of $\sim 75 \mu\text{m}$ are approached with the sharpest indenter already after $\sim 2.25 \text{ mm}$, that means, after the same sliding distance which is found to correspond to the onset of adhesive failure mechanism. This result corroborates the hypothesis of failure mechanisms reported in the previous section. As earlier mentioned, the indenter can penetrate the entire coating thickness of the polyurethane coatings when it is deposited on the stiffer and nearly not deformable glass. In this case, the penetration depth corresponds with the effective penetration capability of the indenter inside the coating material, as the glass, being not compliant at all, is nearly unaffected by the concentrated load of the indenter. Accordingly, after 2.25 mm sliding distance, that is, after 22.5 N applied normal load, the indenter moves across the whole coating thickness, thus approaching the underlying glass. At this point, the indenter acts like a cutting tool, thus generating the layer breakage and the adhesive failure of the overlying coating. This mechanism determines the onset of the linear furrow on the coating surface as depicted in Figure 1(a). The additional damage mechanism can be also associated with the onset of the branch of the penetration depth

characterized by recurrent ridges [Figure 4(a)]. The analysis of the residual depths in Figure 4 provides further indications. They nearly follow a linear increasing trends with a small decreasing branch at the end of the residual scratch pattern, which is ascribable to the aforementioned front pileup. Residual depths are apparently unaffected by the role of the substrate stiffness and compliance. They keep very low whatever the polyurethane coatings are deposited on glass or polycarbonate. When the sharpest indenter tip is used, the maximum residual penetration depth is $\sim 30\text{--}35 \mu\text{m}$. Instead, when the bluntest indenter tip is used, the maximum residual penetration depth is a mere $\sim 5\text{--}10 \mu\text{m}$. Indeed, despite the polyurethane coatings deposited on polycarbonate are susceptible of larger deformation, when submitted to the incremental load during the progressive mode scratch tests, a large share of the imposed deformation charges the underlying polycarbonate. As said, polycarbonate is an extremely ductile and flexible material. When it is submitted to concentrated load, it absorbs large part of the imposed deformation and, when the load is released, it is able to recover most of the accumulated deformation in the elastic field. Accordingly, no history of the previously imposed deformation remains in the substrate material. This is therefore the reason why the polyurethane coatings get the same residual deformation regardless they are deposited on the highly compliant polycarbonate or on the stiffer and nearly not deformable glass. Differently from what happens during the application of the scratch loads and the analysis of the corresponding penetration depths, the final deformation, that is, the permanent one mostly depends on the property of the surface overlying coatings and on loading conditions. Substrates have a minor role on that. In Figure 5, the deformation responses of the thicker $\sim 150 \mu\text{m}$ coatings are reported. The maximum penetration depth depends on the tip radius of the indenter, as well. The trends of the penetration depth are always increasing and keep following an approximately power law. The penetration depth depends on the intrinsic properties of the coating and substrate material, as well. However, when the thicker polyurethane coatings are deposited on polycarbonates, the maximum depth of penetration under the sharpest $100 \mu\text{m}$ tip radius indenter is always $\sim 140 \mu\text{m}$. These results confirm the aforementioned hypothesis according to which, a large share of the plastic

deformation which is measured during the application of the load in the progressive mode scratch tests, is ascribable to the high compliance of the underlying polycarbonate. In fact, the increase in the thickness of the overlying polyurethane coatings does not affect the penetration depth. The increased thickness of the coating is only acting as a relieve layer to transfer the imposed load and the resulting deformation to the farther polycarbonate, which accomplishes the dynamic action of the concentrated load and deform accordingly. In the case of blunt contact condition with the 800 μm tip radius indenter, the measured maximum penetration depth of the polyurethane coating on the polycarbonate is 80–85 μm as in the case of the thinner coatings, as well. The deposition of thicker coating is, however, beneficial on the stiffer and not compliant glass. When it is indented with the sharpest tip, the polyurethane coatings on glass are characterized by a maximum penetration depth which averages $\sim 100 \mu\text{m}$, next to the overall coating thickness. The maximum penetration depth in case of the blunt contact condition with the 800 μm indenter is, instead, 45–50 μm . As said, the glass is stiff and nearly not deformable. The thicker coating is thus beneficial as it is potentially able to absorb more of the imposed deformation by the indenter during the progressive mode scratch tests. The polyurethane coatings average higher penetration depths when thicker and, thus, they are also able to better withstand the penetrating action of the indenter and prevent it to damage the coating. In particular, no C-shaped fractures or adhesive failures are detected on thicker polyurethane coatings [Figure 2(a)] when deposited on glass. This result can be obviously ascribed to the extra amount of material deposited on the stiff glass, which acts as a relieve layer for the stress field imposed by the penetrating indenter on the coating surface. The analysis of the residual depths in Figure 5 confirms the measured values are substantially unaffected by the role of the substrate stiffness and compliance. The maximum residual depths average values close to the ones measured on the thinner coatings, when the sharpest indenter tip is used. Instead, when the bluntest indenter tip is used, the maximum residual penetration depth is nearly negligible. This is the result of the thicker coatings which contribute to absorb the imposed stresses of the indenter, thus leading to a nearly complete recover of the scratch deformation after the load release as shown in Figure 2(b–f).

Analysis of the Wear Response

Wear volume of coatings and, especially, of polyurethane coatings, is generally minimally affected by the intrinsic properties of the underlying substrate. This behavior is confirmed by the polyurethane coatings deposited on glass and polycarbonate, with wear volume which increases similarly with the sliding distance (Figure 6). Observing the trends of the wear volume, the wear rate follows two stages: (i) a first stage during which the material removal is linearly increasing with a moderate wear rate and (ii) a second stage during which the material removal is sped up with a pretty high wear rate. However, after 1000 m sliding distance, the polyurethane coatings deposited on both glass and polycarbonate are still firmly anchored on the underlying substrates, although a lot of the initial material was worn out.

The trends of material loss during the tribological tests and the analysis of the morphological features of the residual wear pat-

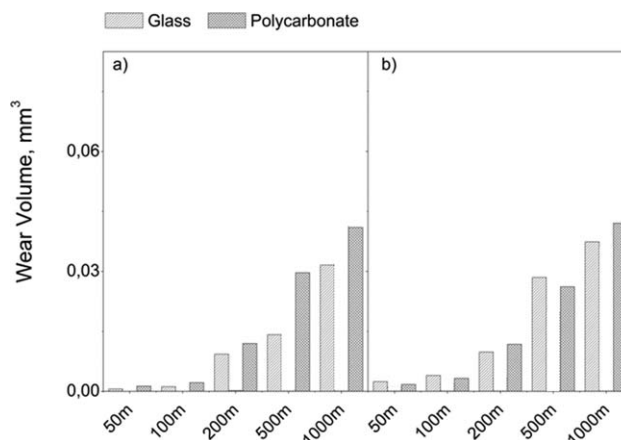


Figure 6. Wear volume during tribological tests performed on the thinner (a) and thicker (b) polyurethane coatings deposited on glass and polycarbonate.

tern suggest the presence of two interaction mechanisms between the coatings investigated and the counterpart: (i) a first step during which very slow material removal is involved and interaction between coating surface and counterpart is essentially governed by friction law and (ii) a second step involving faster material removal, with the formation of debris according to the establishment of concurrent wear mechanisms. During the former step, the interaction by friction can be ascribed to adhesion, that is, to the breaking of adhesive bonds occasionally formed between the coatings and the counterpart and, above all, to ploughing, that is, to the resistance originating from elastic and possibly plastic deformation generated by the action of the counterpart when it slides on the surface of coatings supported by the substrate (i.e., the thin and thick polyurethane coatings on the stiffer glass or on the highly compliant polycarbonate). The coating is thus subject to significant deformation, at least, in the elastic field even when submitted to moderate contact pressure (as it is the case of the initial step of the progressive mode scratch tests), especially on the highly flexible polycarbonate. Accordingly, ploughing is the main friction mechanism. The resulting residual wear pattern is thus influenced by the deformation of the samples during the tribological tests. The polyurethane coatings on polycarbonate deform much more. Despite this would produce an increase in the contact surface between coating surface and interface, it causes a corresponding reduction in the contact pressure. Thus, the coating material is worn out along a narrower stripe as shown in Figures 7(a) and 8(a), that is, whereas the contact pressure is sufficiently high to activate significant wear phenomena. Despite the contact pressure might be lower on average, the contact surface is highly deformed and, thus, susceptible of stronger shear forces once set the normal applied load during the tribological tests [Figure 9(a)]. These stronger shear forces explicate their action mostly on the outermost layer of the coatings, thus leading to material removal which is pretty easily torn off from the bulk of the coatings in the form of large detaching asperities, as clearly seen in Figures 7(a) and 8(a). The polyurethane coatings on glass deform less. This would contribute to increase the contact pressure at the interface between coating surface and

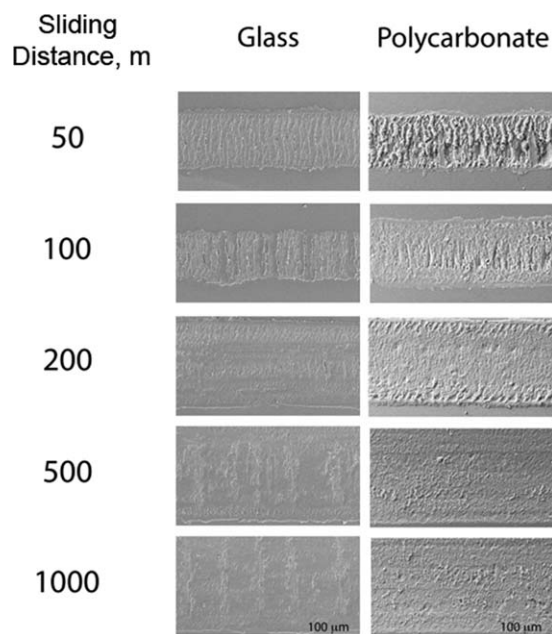


Figure 7. Residual wear patterns at different sliding distance during tribological tests performed on the thinner $\sim 75 \mu\text{m}$ polyurethane coatings deposited on glass and polycarbonate.

counterpart. The coating material is thus worn out along a wider stripes as shown in Figures 7(a) and 8(a), that is, whereas the contact pressure is sufficiently high to activate significant wear phenomena. Nevertheless, as the contact surface between polyurethane coatings deposited on glass and counterpart is less deformed during the tribological tests [Figure 9(b)], the corresponding coating surface is locally susceptible of lower shear forces once the normal applied load is set. These weaker shear

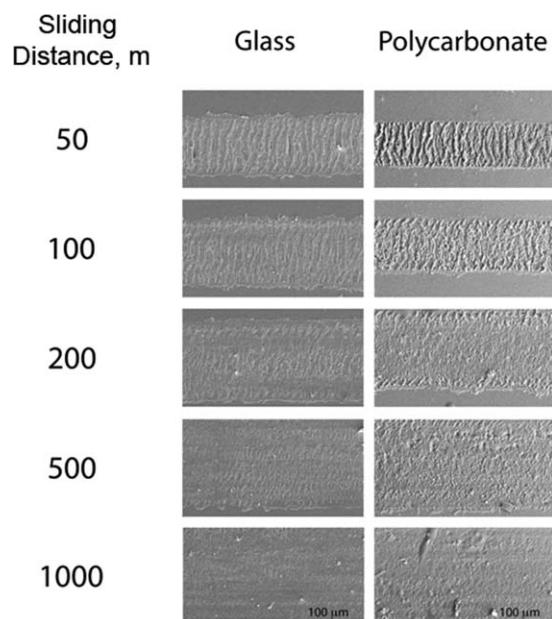


Figure 8. Residual wear patterns at different sliding distance during tribological tests performed on the thicker $\sim 150 \mu\text{m}$ polyurethane coatings deposited on glass and polycarbonate.

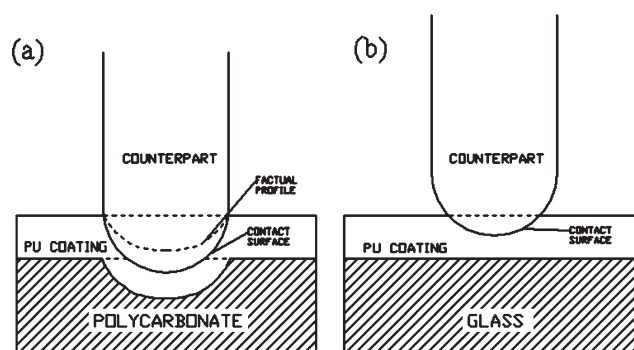


Figure 9. Interaction between counterpart and polyurethane coatings during the dry sliding linear reciprocating tribological tests: (a) polycarbonate and (b) glass.

forces explicate slowly their action on the outermost layer of the coatings, thus leading to a softer material removal and to the formation of smaller detaching asperities, as shown in Figures 7(a) and 8(a). Increasing the sliding distance tends to hinder the different interactions mechanisms between counterpart and coatings deposited on the different substrates [Figures 7(b–e) and 8(b–e)]. However, during the second stage of wear, that is, the one involving the faster material loss, the mechanisms should be similar, with both adhesion and ploughing causing faster material removal along the wear pattern (Figures 7 and 8). Indeed, the material removal might be ascribed to both adhesion + fracture and abrasion + fracture mechanisms as shown in Ref. 14. The counterpart can determine, during its sliding motion, an adhesive lifting and/or a significant deformation in the underlying coating from which shear stresses much higher than the intrinsic strength of the coating material itself can arise. The shear stress can thus cause the onset of surface fractures and, in turn, the formation of debris.

SEM images of the damage of the coating surface by wear further clarify the involved mechanisms. Ploughing and abrasion + fracture are the main mechanisms which are found to cause the material removal from the coating surface during the tribological tests (Figures 7 and 8). In fact, although the typical reciprocating motion of the counterpart on the coating surface should obliterate the material removal mechanisms, SEM images reveal the formation of fractures takes place basically by brittle tensile cracking (Figures 7 and 8). Fractures are C-shaped cracks looking the advancing direction of the counterpart (i.e., the motion of the counterpart is reciprocating and the presence of both leftwards and rightwards C-shaped cracks can be distinguished as shown in Figures 7 and 8). Furthermore, the wear pattern is not characterized by the presence of significant permanent deformation. The C-shaped cracks on the surface with the lack of permanent deformation on the coating underline an elastic brittle response of the coating material during the tribological tests. Therefore, material removal can be essentially attributed to the mechanism of ploughing in the elastic field, that is, to the abrasion + fracture wear mechanism. Friction by adhesion and the corresponding wear mechanism by adhesion + fracture play, if any, only a minor role as also stated in Ref. 14.

CONCLUSIONS

The present investigation focuses on the application of high-clarity polyurethane coatings on transparent glass and polycarbonate. In particular, the role of the coating thicknesses and, above all, of the different compliance of the substrates was investigated.

The following conclusions can be drawn:

- The compliance of the substrate is very influential in determining the scratch performance of the surface overlying coatings: stiffer and poorly deformable glass substrate can be the cause of major failure of thin polyurethane coatings.
- Failure of thin polyurethane coatings on stiff glass can take place by concurrent brittle tensile cracking and adhesive failure, with the latter mechanism being ascribable to the establishment of a true contact between the penetrating indenter and the coating–substrate interface.
- The residual deformation after progressive mode scratch tests of polyurethane coatings deposited on glass and polycarbonate is minimally influenced by the coating thickness and, above all, by the intrinsic properties of the substrate provided that thick enough coatings are deposited.
- Wear rate of the polyurethane coatings followed two stages: (i) a first stage during which the material removal is linearly increasing with a low to moderate wear rate and (ii) a second stage during which the material removal is sped up with a pretty high wear rate.
- The different deformation, the polyurethane coatings deposited on glass and polycarbonate underwent, was found to alter the way by which the material is removed during the dry-sliding contact with the counterpart, with the coating on polycarbonate being submitted to lower contact pressure and high shear forces at the interface substrate counterpart.
- Material removal during wear of the polyurethane coatings can be mostly attributed to the mechanism of ploughing in the elastic field, that is, to the abrasion + fracture wear mechanism, with the friction by adhesion and the corresponding wear mechanism by adhesion + fracture playing a minor task.

The experimental findings allowed to better interpret the way to ruptures of the investigated coating systems during scratch and tribological tests and the corresponding mechanisms involved. Accordingly, new strategies to prevent coating failures and viable solutions to the design and manufacturing of high-resistant polyurethane coatings on compliant and not substrates could be drawn out.

REFERENCES

1. Noble, K. L. *Prog. Org. Coat.* **1997**, *32*, 131.
2. Melchior, M.; Sonntag, M.; Kobusch, C.; Jürgens, E. *Prog. Org. Coat.* **2000**, *40*, 99.
3. Madbouly, S. A.; Otaigbe, J. U. *Prog. Polym. Sci.* **2009**, *34*, 1283.
4. Chattopadhyay, D. K.; Raju, K. V. S. N. *Prog. Polym. Sci.* **2007**, *32*, 352.
5. Barna, E.; Bommer, B.; Kürsteiner, J.; Vital, A.; Trzebiatowski, O. V.; Koch, W.; Schmid, B.; Graule, T. *Compos. Part A: Appl. Sci. Manuf.* **2005**, 473.
6. Liu, L. M.; Qi, Z. N.; Zhu, X. G. *J. Appl. Polym. Sci.* **1999**, *71*, 1133.
7. Cho, J. D.; Ju, H. T.; Hong, J. W. *J. Polym. Sci. Part A: Polym. Chem.* **2005**, *43*, 658.
8. Taylor, S. R.; Sieradzki, K. *Prog. Org. Coat.* **2003**, *47*, 169.
9. Barletta, M.; Pezzola, S.; Trovalusci, F.; Vesco, S. *Prog. Org. Coat.* **2013**, *76*, 1494.
10. Bull, S. J. *Surf. Coat. Technol.* **1991**, *50*, 25.
11. Jardret, V.; Zahouani, H.; Loubet, J. L.; Mathia, T. G. *Wear* **1998**, *218*, 8.
12. Bautista, Y.; Gomez, M. P.; Ribes, C.; Sanz, V. *Prog. Org. Coat.* **2011**, *70*, 358.
13. Jiang, H.; Browning, R. L.; Hossain, M. M.; Sue, H.-J.; Fujiwara, M. *Appl. Surf. Sci.* **2010**, *256*, 6324.
14. Holmberg, K.; Ronkainen, H.; Laukkanen, A.; Wallin, K. *Surf. Coat. Technol.* **2007**, *202*, 1034.